

# **Registering MR Images with Histological Sections using Vascular Landmarks: Part II**

Reza Hosseini

Faculty: Dmitri Artemov (PI), Meiyappan Solaiyappan

EN 520.800.12 – spring 2008

Independent Study

Advisor: Jerry Prince

Spring 2008 Report

## Introduction

This report will review the background and significance for this project and the goals and work finished towards achieving those goals up to a point at which the project's responsibility will be taken by the principal investigator. Progress during the second semester was limited due to various setbacks which will be described in detail throughout this report. The following is a review of the project motivation.

The field of medical imaging as it pertains to tumor models remains relatively unexplored when compared to models such as the heart and brain. However, with the large amount of ongoing research in cancer, there exists a critical need for proof of concept of cancer therapy in tumor models.

In order to validate cancer research, in-vivo images must be compared to histology images. Currently there exists no method for automatic registration of 3D MRI data with 2D serial stacks of histology data (16). Such an application would allow for direct inspection of both data sets simultaneously while correlated to each other. This would allow validation of newly developed cancer or tumor agents.

For example, it can be determined whether new blood vasculature contrast agents are accurate in delineating tumor blood vessels in 3D MRI by comparing to stained blood vessels in microscopy images of the same tumor. This application highlights the emerging need for an automatic registration technique to allow for this comparison and subsequent validation. A major advantage of such a technique is that it could benefit several other cancer studies that focus on various cancer agents which produce marked changes in some form of in-vivo imaging and which can also be viewed with ex-vivo imaging. In our study, once the efficacy of the vasculature contrast agent is confirmed with such a method, it can potentially be used for non-invasive cancer imaging in patients. This data would allow for more accurate and detailed imaging of the tumor and therefore, better effective treatment with more accurate measurement of the response.

3D MRI and 2D histology data has been collected from in-vivo mouse models and subsequent excision of the tumors. This data will be used to create and test an automatic registration algorithm. One of the major goals of this study is to produce a working program, preferably in IDL (Interactive Development Language) programming environment, which automatically finds the best possible 3D co-registration of the volumetric MRI and planar microscopy image data. The novelty of our approach is that we use existing blood vessels as endogenous markers rather than utilizing artificial fiduciary markers or excessive preparation and treatment of the tumors as is done in with existing methods (17, 19, 20). The program will process the original MRI and microscopy data to produce a set of registered images which can then be viewed by visualization programs such as Amira to inspect and validate the results of the co-registration.

Through this method, the efficacy of the blood vasculature contrast agent can be more accurately confirmed while simultaneously providing a means of registration to histology. This new method of utilizing the contrast agent for solving the complex problem of registering 3D volume to 2D planar data can be readily extended to other tumor imaging modalities where conventional methods of registration fail due to lack of symmetry (19) and endogenous markers.

## Goals

MR imaging (MRI) provides highly informative high-spatial resolution imaging of living objects. However to validate the extensive morphological and functional information obtained from MR images histopathological endpoint examination of tissue slices prepared from the organ of interest is typically required. Histological tissue slices imaged with microscopic resolution produce large two-dimensional data sets, which need to be registered with MR maps that have significantly lower (by orders of magnitude) digital resolution. Moreover, histological sections often have distorted boundary areas and possible tissue deformation during the fixation and sectioning procedures. A traditional registration method relies on image analysis of unique morphological features of the tissue and/or application of external fiducial markers visible both in MR images and in histological sections. Unfortunately both approaches have significant restrictions as many important organs of interest do not have required morphological features and external markers can be displaced or often cannot be stably positioned next to the volume of interest.

In this application we intend to use tissue vasculature as a convenient endogenous internal reference marker for registration of MR images with histological sections. Blood vessels are easily identifiable in MR images using an appropriate contrast enhanced acquisition with injectable contrast agents or using endogenous contrast due to the blood flow. Blood vessels can also be routinely stained in histological sections using specific vascular probes or by perfusion of the animal with a fluorescent dye.

Hypothesis: Vasculature can be used as a specific endogenous marker for registration of MR images with histological sections using computer based analysis of MR angiograms (MRA) and the sections with visualized positions of blood vessels. The experiments designed and performed to test this hypothesis will be discussed later.

We have two specific aims to test the hypothesis.

Specific Aim 1: Develop a computer algorithm for automated analysis and registration of 3D MRI data sets and 2D digitized histological sections using an image feature analysis algorithm invariant to rotation and shift transformations. The algorithm will automatically analyze pre-contrast and post-contrast 3D MR images and segment enhanced blood vessels to generate a 3D MRA map. Digitized histological

sections with stained vasculature will also be analyzed, positions of the blood vessels will be mapped, and an invariant digital signature will be generated by the program for the histological slice from the positions of blood vessels. A specialized, operator independent, algorithm will be used to search through the 3D MRA data set and choose a section that has the digital signature closest to that of the histological data set. Once the best candidate section from the MR set is chosen an additional affine transformation can be applied to provide precise co-registration between MR and histological data sets. Preliminary work for this goal is discussed below, and was limited to what is shown due to the unavailability of a complete data set. Most time in the last few months was spent on obtaining a complete study data which was not achieved as discussed below.

Specific Aim 2: Test the MRI/histology registration method based on the positions of blood vessels for an experimental model of human breast cancer growing in severe combined immune-deficient (SCID) mice. The preliminary studies were done with a rat prostate cancer cell line (MatLyLu) due to several attractive qualities such as: aggressive, fast growth of tumors from inoculation, and well vascularized tumor tissue. This allowed experiment time to be greatly shortened from cell culture to histology sectioning. This was ideal for optimizing several aspects of the protocol including, which contrast and fluorescence agents to use.

Tumor bearing animals were scanned on a high-field animal MR scanner ( $B_0=9.4T$ ) with high molecular weight albumin-GdDTPA blood pool contrast media to generate high-resolution 3D angiograms with uniform spatial resolution of about 125  $\mu m$ . To visualize vasculature in the histological sections the animal were infused with a fluorescent, Dextran-based, vascular marker. The marker was changed to an alternative, Dextran-FITC (fluorescein isothiocyanate) conjugated, high molecular weight, agent which provided a better vascular map in histology. The tumor was sectioned on a cryostat and representative sections will be digitized with a fluorescent microscope interfaced to a CCD camera. Histological and MRA images were processed with the registration software to (i) generate a slice from the 3D MR image that corresponds to the histological section and (ii) to apply an affine transformation to the slice(s) for precise registration between MRI and histological data. Performance of the algorithm in determining the precise position of the histological section relative to the MR data set will be evaluated using an independent, gold standard, approach with fiducial markers attached to the tumor surface.

We anticipate that the developed method will provide a direct and reliable approach to register histological and MR data that will have broad applicability to preclinical studies and can also be translated to the clinic using established MRA procedures and specific histological staining of the vasculature in tissue sections.

## Preliminary Studies (continued)

To demonstrate feasibility of the experimental techniques to generate data sets for registration analysis, we performed MR imaging and histological studies with cancer models grown in immune-deficient mice. Highly aggressive and hormone-independent rat prostate cancer cell line, MatLyLu, was used in preliminary studies. Briefly, 1 million tumor cells were injected subcutaneously in the left flank of a male SCID mouse and allowed to grow for a period of 1 to 2 weeks until the tumor reached the size of about  $0.5 \text{ cm}^3$ . During this time all animals were constantly monitored for tumor growth and general health conditions. As MatLyLu tumors are highly invasive and metastatic, all animals with the tumor volume exceeding  $1 \text{ cm}^3$  were sacrificed as recommended by the veterinarian services of JHU.

Tumor bearing mice were anesthetized and imaged on a 9.4T horizontal-bore, small animal MR scanner (Bruker, Biospec) using a home-made gap-loop RF resonator for tumor imaging. The tail vein of the animal was catheterized for intravenous administration of the contrast agent. The imaging protocol included initial tri-planar scout imaging to determine the position of the tumor and to perform graphic prescription for high-resolution 3D MR scans. High-molecular weight MR contrast agent, albuminGdDTPA, prepared as described elsewhere (14) was used for 3D MR angiography (MRA) studies. The agent molecule contains about 19 GdDTPA groups attached to a bovine serum albumin (BSA) backbone, has a molecular weight of approximately 80 kDa, and has a plasma life time of several hours in mice (30). MR acquisition was performed with a 3D fast spin-echo pulse sequence with the following experimental parameters: effective echo time (TE) of 40ms, repetition delay of 250ms, RARE factor (number of spin echo signals per scan) of 8, field of view (FOV) of  $16 \times 16 \times 8 \text{ mm}$ , and acquisition matrix size of  $128 \times 64 \times 32$  for a uniform spatial resolution of  $125 \mu\text{m}$  with zero-filling in both phase encoding dimensions. The total acquisition time with 4 averages was about 5 minutes. Pre-contrast MR imaging was performed before administration of the agent and post-contrast images were obtained starting 3 minutes after intravenous injection of 0.2ml, 60 mg/ml solution of albumin-GdDTPA in saline. The contrast agent was injected via the tail vein catheter without removing the animal from the magnet and changing the tumor position. Albumin-GdDTPA blood-pool agent induces strong positive T1 contrast enhancement in the perfused vasculature causing the blood vessels to be brighter than other tissues. 3D angiograms were generated by simple subtraction of pre-contrast images from post-contrast MR images. All data processing was performed with dedicated Amira and IDL-based image analysis software.

Following post-contrast imaging, the mice were injected intravenously with 0.1ml of 0.5mg/ml Dextran-FITC fluorescent vascular marker for optical fluorescence imaging. Following a circulation period of 20 minutes, the mice were sacrificed and the tumors dissected. The tumors were then fixed in 4% para-formaldehyde, washed, saturated with concentrated sucrose solution, and frozen for cryo-sectioning. Ten micron histological sections were obtained with a cryostat, cell nuclei were

counterstained with Hoechst 33321 blue dye. Mounted sections were imaged with a Nikon fluorescent microscope equipped with a chilled monochrome CCD camera using 4x and 20x objectives. Low magnification images were obtained from different parts of the section with approximately 20% overlap and the combined image of the complete tumor section was reconstructed by an automated tiling of the individual images using a commercial software package.

Typical experimental results for MR angiography and histology for MatLyLu xenografts are shown in Fig. 2.

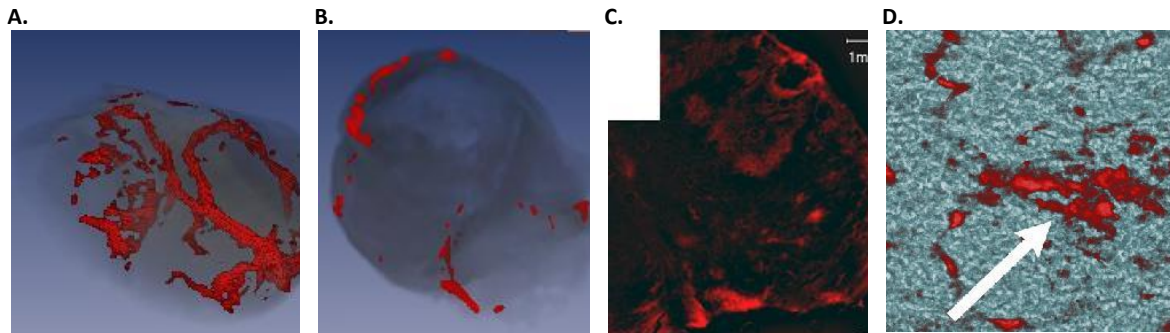


**Figure 2:** (A) Volume rendering presentation of 3D angiograms of a MatLyLu tumor. The tumor blood vessels are rendered using the red color channel; gray color is used for the tumor outline. (B) A 2D section extracted from the 3D MR angiography data set. Blood vessels in the plane are labeled with red color. (C) A fragment from a reconstructed histological slice imaged with 4x objective. Bright red regions correspond to the tumor vasculature stained with Tomato Lectin-TRITC fluorescent marker. (D) Microscopic image of a tumor blood vessel imaged with 20x objective. Lectin-TRITC labeled blood vessels are red.

The prostate rat cancer cell line used in preliminary studies was highly aggressive and reliably produced well vascularized tumors within several weeks of implantation.

The following are further example of MR angiography and histology sections obtained as preliminary results. Several fluorescent agents have been explored in order to determine their efficacy for our purposes. Labels were sought to provide high and clear contrast of the vasculature under low magnification in order to capture an entire tumor section with a single picture. This would simplify the registration process by eliminating prior processing of images including tiling of higher magnification images into an aggregate whole section image. Hoechst, Lectin-TRITC, and Dextran-FITC conjugates have been used as shown in the example below. It can be seen that for our purposes, the Lectin-TRITC marker provides a clear advantage over Hoechst in that a discrete number of blood vessel cross sections can be clearly segmented for use in registration where as in the Hoechst section, there is clear extravasation of the fluorescent label as well as ambiguous areas of fluorescence which make identifying blood vessels difficult. In both cases, low magnification images provided views of the entire section with discernable fluorescence.

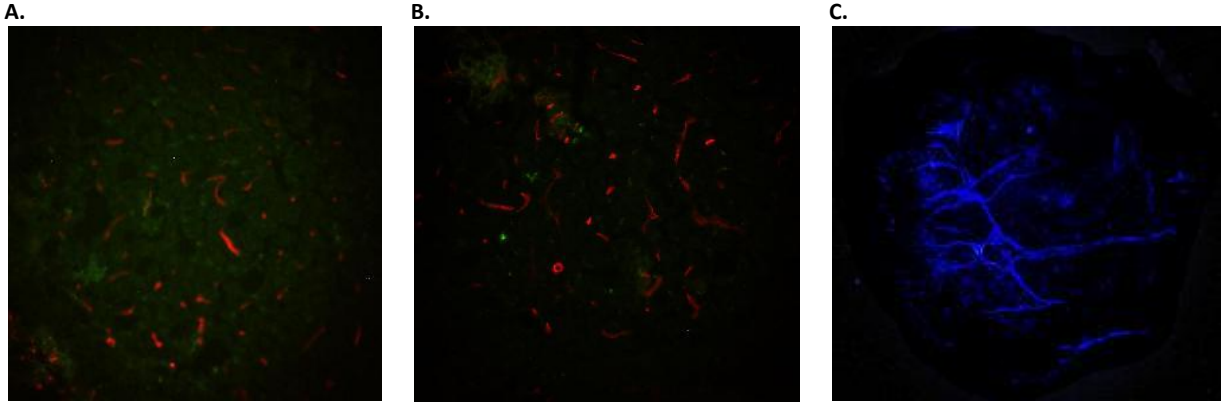


**Figure 3:** Examples of preliminary histology sections with fluorescence. (A), (B) Lectin-TRITC perfused tumor section. (C) Hoechst perfused tumor section. Blood vessels can be seen in all three images, mainly in cross sections but in some areas where the vessel is in line with the cutting plane, there may be a continuous area of fluorescence.

Figure 4 below shows examples of preliminary 3D MRI data sets acquired as described later. Pre and post-contrast images were combined through simple arithmetic operations and a threshold was applied to the result to give the blood vessels seen in figure 4(C). This will serve as the 3D space used for matching a 2D histology slice.

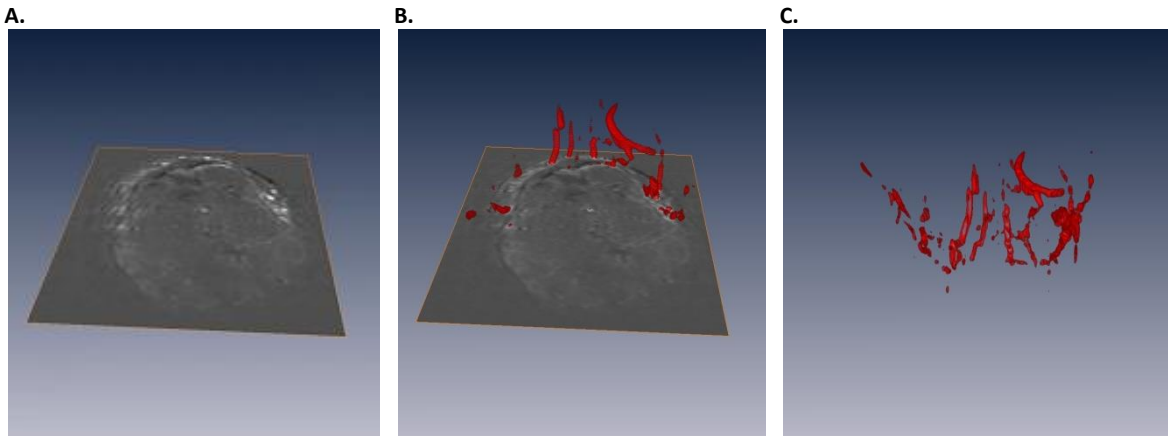


**Figure 4:** Examples of preliminary 3D MRI data sets with GdDTPA contrast enhancement. (A) 2D slice of MRI data set showing post-contrast cross sections of blood vessels near the periphery of the tumor. (B) The same 2D slice shown dissecting the tumor's vasculature after 3D volumetric rendering. (C) 3D stand alone image of whole tumor following pre and post-contrast image subtraction, thresholding, and volumetric rendering.

### Registration of Volumetric MRI and Planar Histological Data

Identifying the best matching image plane in a 3D MRI volume corresponding to the given histological section obtained from the same tumor specimen is a unique challenge that may be approached in various ways. Here we propose a novel approach that maximally exploits the capability of high performance graphics computing

hardware available today to offer an efficient solution that can be flexible enough to benefit other research studies that face a similar problem.

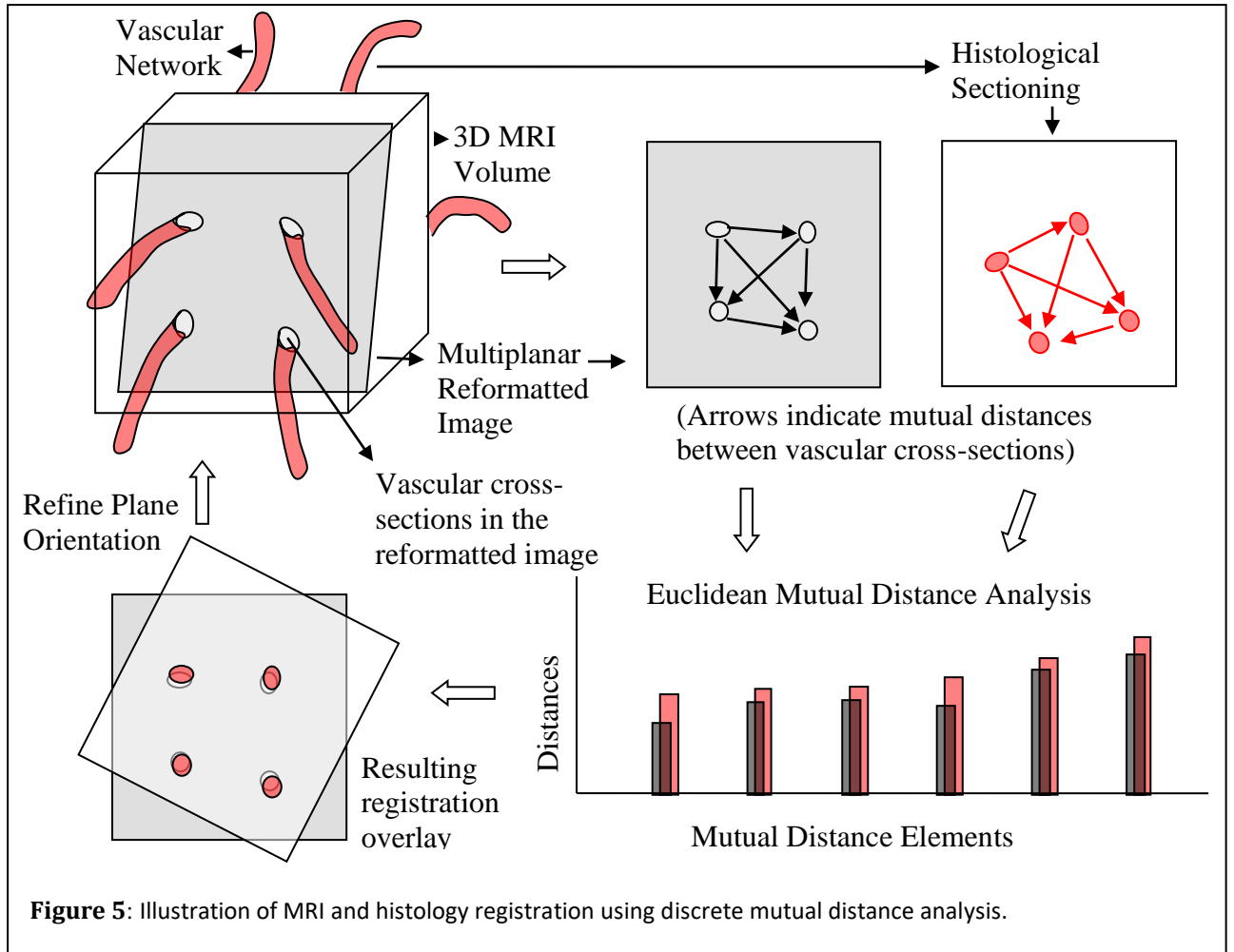


**Figure 5:** Illustration of MRI and histology registration using discrete mutual distance analysis.

The problem involves identifying the transformation which registers the histological section to the 3D MRI volume. Due to the lack of fiducial markers within or around the tumor and the arbitrary orientation of the specimen during histological sectioning and MR imaging, the problem becomes non-trivial. Furthermore, the specimen distortion associated with the preparation for histology and during the subsequent sectioning process can introduce warping that can prevent finding an exact registration. The method presented here can address both of these problems.

Figure 5 provides a general illustration of our approach. We propose to use the mutual distances between the vascular cross-sections in the histology image as a characteristic signature to match with corresponding mutual distances in the multiplanar reformatted (MPR) MRI volume. The major advantage of using mutual distances is that it is invariant under in-plane rotation and translation. Thus it simplifies the problem to three degrees of freedom: matching the position of the MPR image to the

position along the longitudinal axis of the volume and matching the orientation determined by the two angles with respect to the same axis. For the generation of the multi-planar reformatted data we propose the use of high performance graphics cards that support 3D texture mapping. This will facilitate obtaining a MPR image using hardware acceleration. This would make it feasible to generate all possible MPR images closely spaced within the range of variability expected between the 3D MRI data and the histological section. For each of these images, the mutual distances corresponding with the histology can be computed and quantified as described below to determine the best possible match.

The mutual distance analysis involves computing the distances between the centers of each vascular cross section in the MPR data obtained from the MRI volume and comparing them against the mutual distances from the histology data. The deviations between the two sets of mutual distances can be quantified as the sum of the squared differences between nearest matches in the two sets.

For example, if  $d_i^h$  is a mutual distance element in the histology section, then the corresponding pair in MRI is identified by the closest match to  $d_i^h$  as

$$d_j^m = \left[ \left\langle |d_i^h - d_k^m| \right\rangle_{k=1}^{k=N} \right]_{\min}$$

where N is the number of distance elements in the MRI section. The deviation function of the correspondences is then,

$$E_m = \sum_{i=1}^{i=M} (d_i^h - d_j^m)^2$$

where M is the number of distance elements in histology. Computer simulation of a tissue section is shown in Figure 6A and the original and sorted distribution of mutual distances between the centers of blood vessels (red points) in Figure 6B and C respectively.

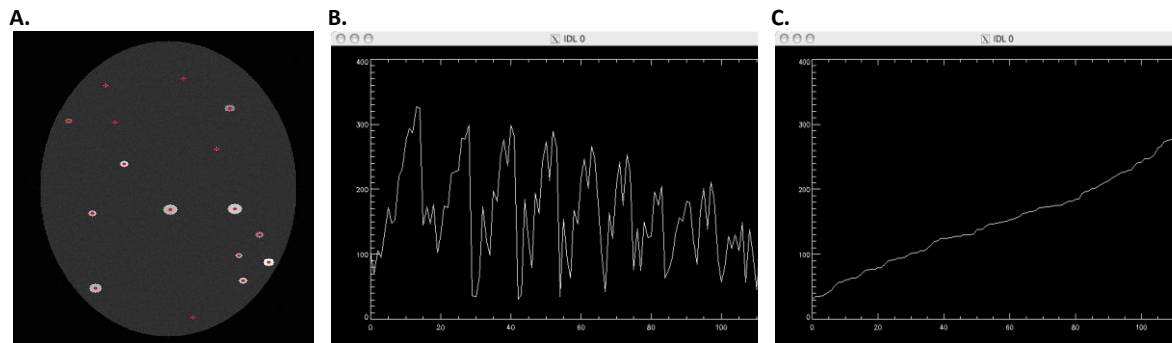


**Figure 6:** Computer simulation of a tissue section with enhanced blood vessels (A) and the corresponding

distribution of the mutual distances plotted vs. pair index (B). (C) The distribution was sorted from the shortest to the longest distance between pairs.

This deviation along with the comparison of the number of distance elements in the two sets M and N can provide the best estimate for the closest match. There may be instances where the mutual distances may have several equidistant pairs from which ambiguous correspondence might arise. However, general randomness in the distribution of the vascular branches could make this a less frequent possibility. When such ambiguities arise, the software can prompt the user to intervene to manually resolve the ambiguity.

The simplicity of the exhaustive search approach to find the best possible correspondence makes it possible to include additional constraints such as the warping factors associated with the histological sections. Since these geometrical distortions are usually a small fraction of the image dimension, they can be taken in to consideration in the distance analysis as a variation of scaling factors for the dimensions of the image within a given range, thereby expanding the search domain for finding the best possible match. The discrete nature of the number of vascular cross-sectional elements is an important factor in the choice of an exhaustive search approach.

The performance consideration of such an approach relies on recent advances in graphics hardware for image computation that provide hardware accelerated multi-planar reconstruction at a fraction of the cost of a supercomputer platform. This will substantially reduce the computational burden of the approach. If processing speed needs to be reduced further, the exhaustive search approach makes the technique highly parallelizable using multi-core low-cost multi-threaded accelerator boards based on GPGPU architecture (General Purpose computing on commodity Graphics Processing Unit) that are becoming popular in solving large scale simulation problems.

## **Research Design and Methods**

*Specific Aim 1. To develop a computer algorithm for automated analysis and registration of 3D MRI data sets and 2D digitized histological sections using an image feature analysis algorithm invariant to rotation and translation transformations.*

The program package will be initially developed using the IDL programming environment. The package will include two major subunits: The first unit will perform initial segmenting of images, determination of image signatures, and choosing the closest matches for a histological section from the 3D MR data set. The basic initial steps will include a low pass filter to reduce high frequency noise and leave only the major contributing blood vessels. The next step involves subtracting the pre-contrast image from the post-contrast image to eliminate as much of the background as possible and leave only the bright vessels. Following this step would be thresholding the pre and post-contrast images to remove as much of the remaining background as possible. This will provide images with only a tumor outline and vasculature in a 3D volume in the case

of MR and 2D in the case of the histology sections to use in the registration. These procedures will be performed with operator involvement limited to the definition of general constraints such as approximate orientation of the histological section and final inspection of several best matches generated by the program. The second unit will perform a rigid and/or affine transformation of the histological section for optimized registration. The block diagram of the algorithm is presented in Figure 7.

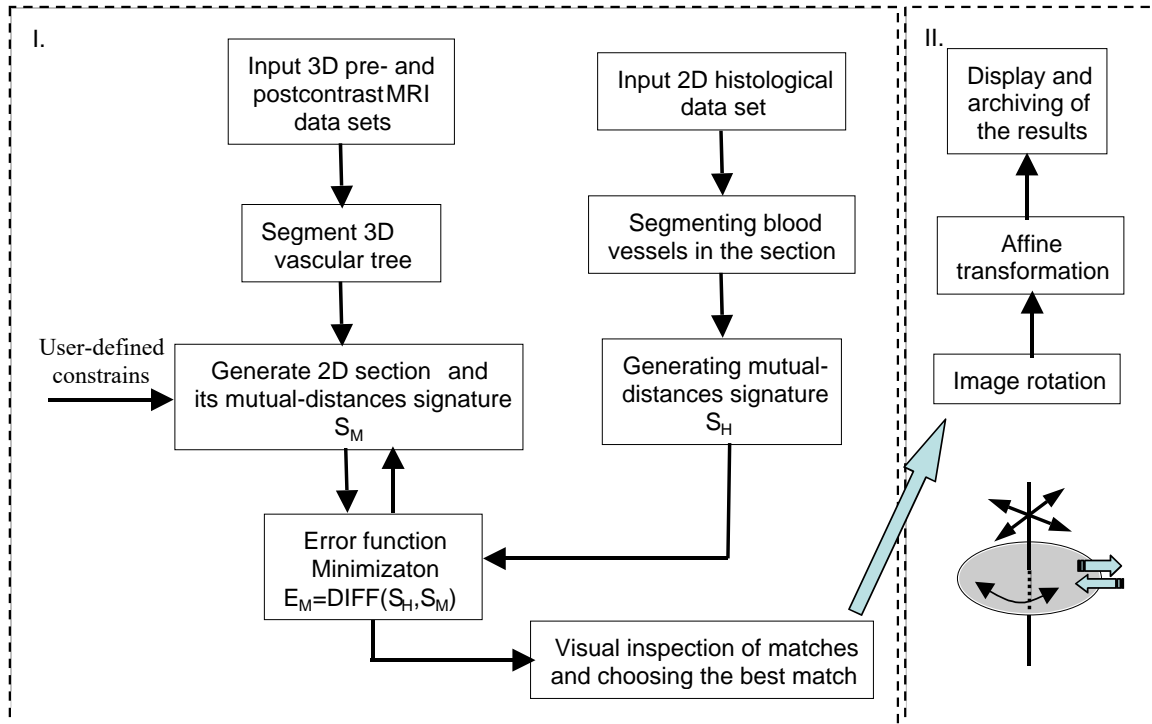


**Figure 7.** Block diagram of the registration algorithm. The two major program units are labeled as (I) and (II).

To exclude possibility of local minima the error function minimization algorithm in Block I initially will use a Monte Carlo based approach. We expect that with increased computing power and appropriate user-defined constrains such as the histology plane orientation, the exhaustive search solution of the problem for  $128 \times 128 \times 128$  MRI data sets with one linear and two angular degrees of freedom should be possible. For the image dimensions of  $128^3$ , the lowest angular separation that will produce detectable difference in the multi-planar reconstruction would be approximately  $\arctan(1/128)$  or 0.45 degrees. So we can choose 0.4 or 0.5 degrees as the step size in both angular dimensions. The total number of possible solutions for sections selected with a unity shift step and leading angles in the range of  $+30^\circ$  to  $-30^\circ$  with 0.4 deg increments from the histology plane orientation will be of about  $128 \cdot 75 \cdot 75 \approx 7 \cdot 10^5$ . Mutual distance analysis will be used to select best matches as described above. The error function will be optimized to produce a limited number of sections (up to 16) with an acceptable fit for the final evaluation by the operator. The second program subunit will provide final registration of the histological section with an MR slice using linear offsets, in plane

rotation, and linear stretching/skewing of the sections. Again, positions of the blood vessels will be used as reference points to guide the image registration routine.

The method will be initially developed in the IDL programming environment on a multiprocessor Linux based computer system and its performance will be evaluated for simulated and several experimental data sets. IDL has built-in support for multithreaded multiprocessor calculations that significantly improves performance on multiprocessor systems. Once a stable working prototype is developed we will proceed with the development of C++ code that will utilize multi-threaded accelerator boards based on GPGPU architecture. Meiyappan Solaiyappan who has significant expertise in the development of computer applications for processing, visualization, and analysis of multidimensional data will be a key investigator involved in this specific aim. Random artificial data sets will be used to test and troubleshoot the program and to determine reasonable constraints to limit the processing time to about 10-20 minutes with the IDL package running on a Linux workstation with two Intel Xeon 2.80 GHz processors.

*Specific Aim 2. To test the MRI/histology registration method based on the positions of blood vessels for an experimental model of human breast cancer growing in immune-deficient SCID mice.*

All experiments will be performed with the MDA-MB-231 human breast carcinoma, hormone independent model, grown in female immune-deficient SCID mice. Briefly, cancer cells ( $1 \times 10^6$ ) will be transplanted ortho-topically into the top left mammary fat pad of the 8-12 week old mouse via a 27-gauge needle. All procedures will be performed in the sterile environment of a laminar flow cabinet and tumors will be allowed to grow to a volume of 300 mm<sup>3</sup>.

*In vivo* MR experiments will be performed with anesthetized animals, horizontally positioned in a Plexi-glass cradle in the bore of the 9.4T superconducting magnet of a Bruker Biospec MR animal system. Restraining anesthesia for short scans will be provided in the form of a ketamine/acepromazine mixture as described above. For prolonged MRI scans animals will receive inhalation anesthesia of 1% isoflurane in 70% O<sub>2</sub>/ 30% N<sub>2</sub> at a rate of 1 ml/min through a nose mask using anesthesia manifolds. Animal body temperature will be stabilized by a circulating water pad in the MR scanner. The tail vein will be catheterized for intravenous infusion of the contrast agents and rectal temperature will be maintained at 37°C by a circulating water thermo-pad. Respiration of the animal will be monitored with a dedicated physiology monitoring system attached to the MR scanner. All MR measurements will be collected in the clean environment of the animal molecular imaging center. If necessary, the animals will be returned to cages in the clean holding area after completing MR scans where they will be maintained for the duration of the study.

To validate our vascular based approach of image registration, fiducial markers will be used as artificial landmarks for co-registration of MR images and histological sections. Tumors will be shaved and small spheres made of soft silicon rubber will be

attached to the skin at three different locations using Superglue. Signals of soft polymer can be reliably detected with short echo time (TE < 50ms) MR imaging. The tumor with the attached markers will be positioned in a home-built RF resonator and MR scans will be performed as described below. Immediately after completing the imaging study the fiducial markers will be gently removed and the tumor will be labeled using a micro tattoo kit (Braintree Scientific, Inc.). A mixture of green tattoo paste and Hoechst 33342 fluorescent dye will be injected into the surface of the tumor at the positions of the markers via a hypodermic needle to enable optical detection of the marker with visible and UV fluorescent microscopy.

## MR protocol

MR acquisition will be performed with a standard 3D fast gradient-echo pulse sequence using the following experimental parameters: effective echo time of 2.5ms, repetition delay of 8ms, FOV of 18x18x9 mm. This protocol provides sufficient FOV coverage for a typical tumor and results in a uniform spatial resolution of 125  $\mu$ m. Initial image reconstruction will be performed with standard Bruker Paravision software installed on the MR scanner and a dedicated IDL-based software will be used for post-processing of experimental data. Albumin-GdDTPA blood-pool paramagnetic contrast agent will be used for specific enhancement of the blood vessel signals. The imaging protocol is outlined in Table 1.

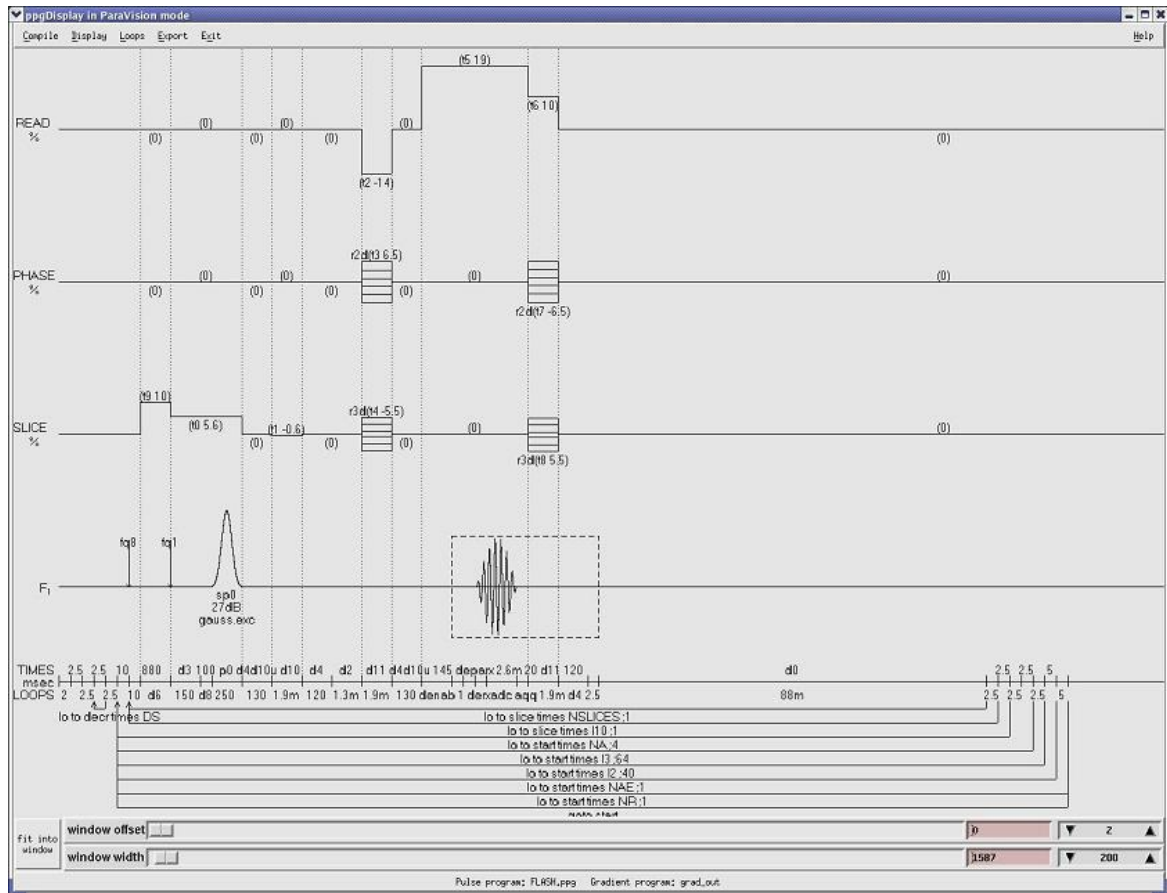
**Table 1.**

<b>Scout Imaging</b> →	<b>Precontrast imaging</b> →	<b>Contrast administration</b> →	<b>Postcontrast imaging</b>
Triplanar MRI with spin-echo sequence is used to generate a dataset for graphical prescription for 3D scan. Imaging time ~ 3min.	Fast gradient-echo 3D MRI. TE/TR = 2.5/8ms, Total imaging time of ~10 min.	0.2 ml of 60 mg/ml solution of albumin-GdDTPA in saline administered i.v. into the tail vein as a bolus. Postcontrast scan starts ~3 min after the bolus to allow equilibration of contrast in the vasculature.	Fast gradient-echo 3D MRI. TE/TR = 2.5/8ms, Total imaging time of ~10 min.

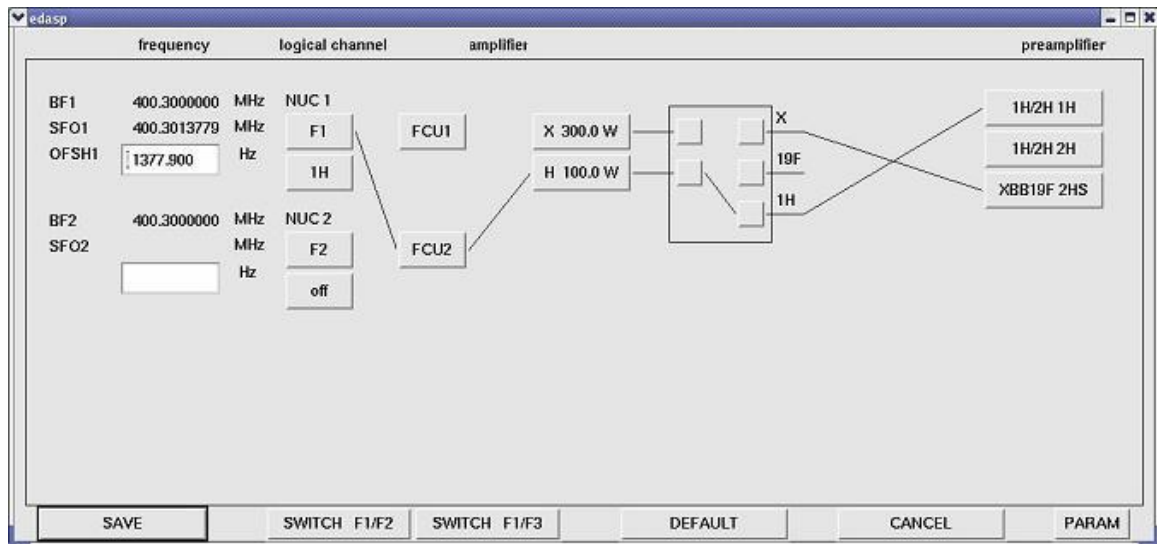
Positions of the fiducial markers will be marked on the tumor surface with the tattoo kit as described. 3D MR images will be reconstructed and 3D angiograms will be generated by subtraction of pre-contrast images from post-contrast MR images with an additional low-pass filtering and an appropriate threshold applied to the difference data. MR signal of the fiducial markers will be manually segmented and saved as corresponding 3D masks that can be added to 3D angiograms for visualization and/or registration with histological slices.

The updated protocol involved only 2 FLASH sequences to be used for pre and post-contrast imaging. The figure below illustrates the pulse sequence with the read,

phase, and slice encoding gradients, timing, and RF signals. Repetition time is approximately 8ms, echo time 2.5ms, 40 degree flip angle which was obtained by reducing the normal 90 degree angle by 7-8dB. This achieved a field of view of 18x18x9mm. We used 4 averages to obtain the data and increase SNR.



A partial flow diagram is also shown below, which was extracted from the Bruker magnet which illustrates the signal flow for the RF excitation and amplification.



The figure below is a snapshot of the Paravision program tools used to configure the scanner before each study. It shows the windows used to shim the magnet, adjust the amplification, receiver gain, attenuation, and reconstruction parameters.

Parameter Editor for RECO\_IN

RECO: processing mode	FT_MODE
RECO: input reordering	NO_REORDERING
RECO: reconstruction size	{ 128, 128, 64 }
RECO: field of view	{ 1,6000, 1,6000, 1,2000 } cm
RECO: output size	{ 128, 128, 64 }
RECO: regrid mode	NO_REGRID
RECO: navigation mode	NO_NAV_DATA
RECO: BC mode	{ NO_BC, NO_BC, NO_BC }
RECO: quadrature options	{ CONJ_AND_QNEG, NO_QOPTS, NO_QOPTS }
RECO: WDW mode	{ SINE, SINE, SINE }
RECO: sine bell shift	{ 1,000, 1,000, 1,000 }
RECO: FT mode	{ COMPLEX_FFT, COMPLEX_FFT, COMPLEX_FFT }
RECO: PC mode	{ NO_PC, NO_PC, NO_PC }
RECO: rotation of data	_expand
RECO: Post-processing PC	NO_PPC
RECO: DC spike elimination	No
RECO: image transposition	{ 1 }
RECO: output image type	MAGNITUDE_IMAGE
RECO: output word size	_32BIT_FLOAT

Spectrometer Control Tool - ParaVision

Basic Frequency BF1 400.301378 Set Basic Frequency

Offset Frq O1 0.0 1.0

Transmitter Setting Channel 1

Tx Attenuator 0 27.0 1.0

Tx Attenuator 1 12.0 1.0

Receiver Setting

Receiver Gain 1200.0 20.0

## **Staining of blood vessels and histology**

Blood vessels will be stained with a fluorescent Dextran-FITC marker as described in Preliminary data. Briefly, after completing post-contrast MR scan, the mice will be injected intravenously with 0.1ml of 1 mg/ml solution of Dextran-FITC fluorescent vascular marker in saline. Following a circulation period of 1-2 minutes, the mice will be sacrificed and the tumors will be dissected and the orientation of head-tail and left-right direction will be marked on the tumor with a lab marker. The whole tumors will be fixed in 4% paraformaldehyde overnight, washed, saturated with concentrated sucrose solution at 4°C, and frozen in liquid nitrogen using a plastic floater to support the tissue above the surface of the liquid. Ten micron histological sections will be cut with a cryostat using coarse orientation parallel to the body wall of the animal and mounted on a glass slide with the head-tail axis parallel to the long side of the slide. In some sections cell nuclei will be counterstained with Hoechst 33321 blue fluorescent DNA dye. Mounted sections will be imaged with a Nikon fluorescent microscope equipped with a chilled monochrome CCD camera using 4x and 20x objectives. Images will be recorded from overlapping segments of the section and the combined image of the complete tumor section will be reconstructed by an automated tiling of the individual images. On each digital image the positions of blood vessels (red fluorescent marker) and surface positions of the fiducial markers (blue fluorescence and green ink) will be manually segmented and saved as 2D masks for image analysis and registration. The vascular staining protocol will be optimized with 3 to 4 animals prior to commencing MR imaging studies. To confirm Dextran-based vascular staining for the model used in the study we will stain several sections with a standard anti-CD34 mAb endothelial marker and will compare the resulting staining patterns.

## **Data processing and analysis**

The computer algorithm developed in Specific Aim 1 of the proposal will be used to analyze 3D MRI data sets and 2D histological slices. Stained blood vessels in the histological section will be manually segmented using a real time subroutine; the vascular tree in 3D MRI data sets will be automatically segmented and presented for inspection by the operator. The operator will also visually inspect MR sections generated by the program and will compare them to the histological slice to choose the best fitting one for the final registration. The relative error of the registration will be reported as a total of squared distance differences as described above. No information regarding positions of the fiducial markers will be used at this point. The quality of registration will be assessed using segmented signals of the fiducial markers in the histological and MRI maps. We expect that images registered using vascular markers will demonstrate precise co-localization of the fiducial markers.

## **Current Work**

The capabilities of the Interactive Development Language (IDL) computing environment, through the testing of a basic registration algorithm, were explored. The reference space used was a basic 2D coordinate space. A histology image was taken as the first image and the same image was translated and rotated by an arbitrary amount and used as the second image. The images were subsequently compared in this reference frame. The spatial mapping function used to transform the image within the reference frame was a linear shift and rotation. These functions were built in to the IDL library and were rigid transformations. The similarity measure used to compare the two images to determine the accuracy of the registration and the mapping function was a linear Pearson correlation. The optimization algorithm used to search the possible spatial mapping functions to determine which yields the best registration was the Powell method. This method searches each degree of freedom, three degrees in this case (rotation around the z-axis, shift in the x-direction and shift in the y-direction), for the best match and returns the array containing this information. In this case, the Powell method used the linear Pearson correlation as the measure of how well a transformation matches the images and cycles through the possible rotations and shifts until it finds the combination creating the highest correlation between the two images. Here, the image needs to be converted to a 1D array of image values in order for the algorithm to use it. The correlation is found between the two arrays, each representing an image. Powell also takes in a tolerance factor to determine when the best match is found. The algorithm also needs an initial starting direction as well as an initial guess of a rotation and shifts. The algorithm returns the initial guess array, now containing the optimized values for the transformation.

This program was able to successfully register the two images within the provided tolerance factor. However, the inefficiency of the Powell method creates a requirement for a relatively large amount of CPU power and the convergence time was around five to ten seconds. This method would be difficult to use for our application in 3D space with the added complexities. Convergence time would be much larger under these conditions, creating the need for a supercomputer or parallel programming if such methods are to be used.

## **Updated Timeline, and Potential Problems**

1. Developing of the prototype software package in IDL and testing it with model datasets (months 1-6).

Limited progress was made in this area due to several setbacks with the preliminary in-vivo studies to establish a base data set to use for the development of software. The goal was to obtain a total data set from one mouse in order to have consistent data for the 3D MRA and histology after perfusion with a fluorescence agent. A full experiment has not been conducted due to problems with the GdDTPA contrast

agents causing death of the mice within seconds of injection. This was most likely due to errors in the production of the agent which is a multiple step, multiple day procedure. Most likely there was free Gadolinium in the solution, which is toxic to living tissue, and causes an immediate systemic response followed by death. A new batch of contrast agents is being produced and will be tested and filtered before use on live animals.

2. Growing the mouse model of human MDA-MB-231 breast cancer and optimizing Lectin staining protocol for tumor vasculature (months 4-7).

The mouse model using the MatLyLu rat prostate cancer cell line was troublesome due to the extremely aggressive nature of cell proliferation and regeneration. Tumors would grow to small marble size within one week. Due to the fast growth and limited time available on the high field MR scanner, by the time tumors were grown, even a one day shift in imaging ability would result in the tumor being too large to fit in the custom coil required for the 3D imaging. Also, this cancer cell line, modeled erratic growth and asymmetric, multiple-lobed tumors which also made imaging difficult.

3. Testing MRI protocols and imaging of the fiducial markers (months 8-10).

The final protocol was developed to be a 3D fast gradient echo (FLASH) sequence run once prior to contrast enhancement to provide a pre-contrast data set and once again after injection of the contrast agent to provide the post-contrast data set.

4. MRI studies with ~10 animals, preparation of the tumor slices, initial histological examination (months 11-14).

15 animals were ordered throughout the last few months and studied at different intervals. The first set of three animals were inoculated with  $1 \times 10^6$  cells. After counting and diluting cells appropriately to ensure consistent and accurate inoculations, tumor growth was inconsistent, and therefore erratic between the mice inoculated simultaneously with the same number of cells. Only one of the animals was able to be used due to excessive tumor growth restricting the use of the custom built tumor coil. The other mouse died sometime after the pre-contrast scan before injection of the fluorescence agent, for which the mouse needs to be living. The live heart is needed to pump the agent throughout the circulatory system and thus provide sufficient perfusion within the tumor. Upon sacrificing the animal within 1-2 minutes of injection, the cease of blood flow ensures deposition of the agent within the vasculature of the tumor as well as limited extravasation of the agent outside the vessels which can significantly decrease histology quality.

The next three animals were similarly prepared for a new study. This time, injections were staggered in the number of cells but still given at the same time. This was in an effort to provide some predictability to tumor maturity and the ability to scan them on separate days as scanner availability determined. The three mice were inoculated as follows:  $1 \times 10^4$ ,  $1 \times 10^5$ ,  $1 \times 10^6$  cells.

It was with this new three animal study it was determined that the contrast agent was poisonous to the animals. Therefore, this study was also wasted. It was most likely this agent that had caused the previous animal deaths. Due to the long turn around time for synthesizing the contrast agent, this study was also wasted. One of the animals was given a dose of the contrast agent to confirm the toxicity. Upon injection, the animal was observed to instantly seizure and death immediately followed.

The following steps were not undertaken during this time period. The project will be taken over by Dmitri Artemov as the principal investigator.

5. Optimizing the registration algorithm for real imaging/histological data (months 12-15).
6. Developing a highly efficient C++ package that fully utilizes advanced multi-core multi-threaded accelerator boards based on GPGPU architecture (months 15-24).
7. Analyzing data and preparing reports and publications (months 18-24).

Several potential problems that can be encountered include:

- (i) Low number of enhancing blood vessels in the tumor model used in the study may limit precision of registration for an arbitrary histological plane. We have chosen a tumor model that is characterized by relatively high blood volume (15). Acquiring MR images with higher spatial resolution achieved by reducing the number of repetitions and/or increasing the imaging time can improve visualization of the vasculature. The total imaging time is limited by slow extravasation of the albumin-GdDTPA contrast agent in the tumor that can potentially reduce imaging contrast for blood vessels.
- (ii) Dextran-FITC staining of the tumor vasculature may not provide sufficient sensitivity for reliable detection of the vasculature at low magnification (4x – 10x). To improve detection of the blood vessels in histological sections we can use bright UV fluorescent Hoechst 33342 dyes that have been widely used for staining the vasculature (9). To minimize the leakage of the dye from the blood vessels the timing of the injection of the probe and sacrificing the animal should be carefully optimized. Also we can acquire images with higher magnification (20x) using a dedicated system available at the JHU Microscopy core facility equipped with an automatic positioning and shutter devices to prevent the excessive photo-bleaching of the sample by prolonged fluorescence measurements. Fluorescein isothiocyanate-dextran (Dextran-FITC) was tested for better

histological results. The molecular weight and chemical properties were optimal for our purposes. Vessel leakage was less likely with this marker.

(iii) Performance of algorithms written in macro IDL language can be suboptimal for practical applications of the method. We will evaluate performance of the procedure using simulated datasets early in the project. If low performance figures are encountered we will develop the program using lower level C++ programming that typically provides significantly improved computational performance.

## References

1. Dauguet, J., Delzescaux, T., Conde, F., Mangin, J. F., Ayache, N., Hantraye, P., and Frouin, V. Three-dimensional reconstruction of stained histological slices and 3D non-linear registration with in-vivo MRI for whole baboon brain. *J Neurosci Methods*, *164*: 191-204, 2007.
2. Breen, M. S., Lazebnik, R. S., and Wilson, D. L. Three-dimensional registration of magnetic resonance image data to histological sections with model-based evaluation. *Ann Biomed Eng*, *33*: 1100-1112, 2005.
3. Kiessling, F., Le-Huu, M., Kunert, T., Thorn, M., Vosseler, S., Schmidt, K., Hoffend, J., Meinzer, H. P., Fusenig, N. E., and Semmler, W. Improved correlation of histological data with DCE MRI parameter maps by 3D reconstruction, reslicing and parameterization of the histological images. *Eur Radiol*, *15*: 1079-1086, 2005.
4. Zhang, H., Maki, J. H., and Prince, M. R. 3D contrast-enhanced MR angiography. *J Magn Reson Imaging*, *25*: 13-25, 2007.
5. Fink, C., Goyen, M., and Lotz, J. Magnetic resonance angiography with blood-pool contrast agents: future applications. *Eur Radiol*, *17 Suppl 2*: B38-44, 2007.
6. Lin, H. Y., Dale, B. M., Flask, C. A., and Duerk, J. L. Blood attenuation with SSFP-compatible saturation (BASS). *J Magn Reson Imaging*, *24*: 701-707, 2006.
7. Miraux, S., Franconi, J. M., and Thiaudiere, E. Blood velocity assessment using 3D bright-blood time-resolved magnetic resonance angiography. *Magn Reson Med*, *56*: 469-473, 2006.
8. Pusztaszeri, M. P., Seelentag, W., and Bosman, F. T. Immunohistochemical expression of endothelial markers CD31, CD34, von Willebrand factor, and Fli-1 in normal human tissues. *J Histochem Cytochem*, *54*: 385-395, 2006.
9. Ching, L. M., Zwain, S., and Baguley, B. C. Relationship between tumour endothelial cell apoptosis and tumour blood flow shutdown following treatment with the antivascular agent DMXAA in mice. *Br J Cancer*, *90*: 906-910, 2004.
10. Raman, V., Artemov, D., Pathak, A. P., Winnard, P. T., Jr., McNutt, S., Yudina, A., Bogdanov, A., Jr., and Bhujwalla, Z. M. Characterizing vascular parameters in hypoxic regions: a combined magnetic resonance and optical imaging study of a human prostate cancer model. *Cancer Res*, *66*: 9929-9936, 2006.
11. Kenwright, C., Bardinet, A., Hojjat, S. A., Malandain, G., Ayache, N., and Colchester, A. C. F. 2-D to 3-D Refinement of Post Mortem Optical and MRI Co-registration. *Medical Image Computing and Computer-Assisted Intervention - MICCAI 2003*, 935-944, 2003.
12. Meyer, C. R., Moffat, B. A., Kuszpit, K. K., Bland, P. L., McKeever, P. E., Johnson, T. D., Chenevert, T. L., Rehemtulla, A., and Ross, B. D. A methodology for registration of a histological slide and in vivo MRI volume based on optimizing mutual information. *Mol Imaging*, *5*: 16-23, 2006.
13. Jacobs, M. A., Windham, J. P., Soltanian-Zadeh, H., Peck, D. J., and Knight, R. A. Registration and warping of magnetic resonance images to histological sections. *Med Phys*, *26*: 1568-1578, 1999.

14. Bhujwalla, Z. M., Artemov, D., Natarajan, K., Solaiyappan, M., Kollars, P., and Kristjansen, P. E. Reduction of vascular and permeable regions in solid tumors detected by macromolecular contrast magnetic resonance imaging after treatment with antiangiogenic agent TNP-470. *Clin Cancer Res*, 9: 355-362, 2003.
15. Bhujwalla, Z. M., Artemov, D., Natarajan, K., Ackerstaff, E., and Solaiyappan, M. Vascular differences detected by MRI for metastatic versus nonmetastatic breast and prostate cancer xenografts. *Neoplasia*, 3: 143-153, 2001.
16. J. V. Hajnal, D. J. Hawkes and D. L. G. Hill, *Medical Image Registration*. Boca Raton: CRC Press, 2001, pp. 382.
17. M. S. Breen, R. S. Lazebnik and D. L. Wilson, "Three-dimensional registration of magnetic resonance image data to histological sections with model-based evaluation," *Ann. Biomed. Eng.*, vol. 33, pp. 1100-1112, Aug. 2005.
18. Y. Guo and Cheng-Chang Lu, "Multi-modality image registration using mutual information based on gradient vector flow," in *Pattern Recognition, 2006. ICPR 2006. 18th International Conference on*, 2006, pp. 697-700.
19. M. A. Jacobs, J. P. Windham, H. Soltanian-Zadeh, D. J. Peck and R. A. Knight, "Registration and warping of magnetic resonance images to histological sections," *Med. Phys.*, vol. 26, pp. 1568-1578, Aug. 1999.
20. C. Kenwright, A. Bardinet, S. A. Hojjat, G. Malandain, N. Ayache and A. C. F. Colchester, "2-D to 3-D Refinement of Post Mortem Optical and MRI Co-registration," *Medical Image Computing and Computer-Assisted Intervention - MICCAI 2003*, pp. 935-944, 2003.
21. F. Kiessling, M. Le-Huu, T. Kunert, M. Thorn, S. Vosseler, K. Schmidt, J. Hoffend, H. Meinzer, N. E. Fusenig and W. Semmler, "Improved correlation of histological data with DCE MRI parameter maps by 3D reconstruction, reslicing and parameterization of the histological images," *Eur. Radiol.*, vol. 15, pp. 1079-1086, 06/12. 2005.
22. C. Liu, K. Li and Z. Liu, "Medical image registration by maximization of combined mutual information and edge correlative deviation," in *Engineering in Medicine and Biology Society, 2005. IEEE-EMBS 2005. 27th Annual International Conference of the*, 2005, pp. 6379-6382.
23. C. Liu, J. Yang, P. Shao, J. J. Gu and M. Yu, "Mean divergence measures for multimodality medical image registration," in *Electrical and Computer Engineering, 2007. CCECE 2007. Canadian Conference on*, 2007, pp. 1171-1174.
24. F. Maes, A. Collignon, D. Vandermeulen, G. Marchal and P. Suetens, "Multimodality image registration by maximization of mutual information," *Medical Imaging, IEEE Transactions on*, vol. 16, pp. 187-198, 1997.
25. C. R. Meyer, B. A. Moffat, K. K. Kuszpit, P. L. Bland, P. E. Mckeever, T. D. Johnson, T. L. Chenevert, A. Rehemtulla and B. D. Ross, "A methodology for registration of a histological slide and in vivo MRI volume based on optimizing mutual information," *Mol. Imaging*, vol. 5, pp. 16-23, Jan-Mar. 2006.
26. M. Moshfeghi, "Multimodality image registration techniques in medicine," in *Engineering in Medicine and Biology Society, 1989. Images of the Twenty-First*

- Century. Proceedings of the Annual International Conference of the IEEE Engineering in, 1989, pp. 2007-2008 vol.6.
27. J. P. W. Pluim, J. B. A. Maintz and M. A. Viergever, "Mutual-information-based registration of medical images: a survey," *Medical Imaging, IEEE Transactions on*, vol. 22, pp. 986-1004, 2003.
  28. J. P. W. Pluim, J. B. A. Maintz and M. A. Viergever, "Image registration by maximization of combined mutual information and gradient information," *Medical Imaging, IEEE Transactions on*, vol. 19, pp. 809-814, 2000.
  29. P. Viola and W. M. Wells III, "Alignment by maximization of mutual information," in *Computer Vision, 1995. Proceedings., Fifth International Conference on*, 1995, pp. 16-23.
  30. Z. Zhang, "A Mouse Model of Embolic Focal Cerebral Ischemia," *Journal of Cerebral Blood Flow & Metabolism*, 1997, 17, 1081-1088.
  31. M. Dreher, "Tumor Vascular Permeability, Accumulation, and Penetration of Macromolecular Drug Carriers," *Journal of the National Cancer Institute*, Vol. 98, No. 5, March 1, 2006.